Supporting Information:

Can Local Heating and Molecular Crowders Disintegrate Amyloid β_{17-42} Aggregate?

Naresh Kumar,[†] Prabir Khatua,[‡] and Sudipta Kumar Sinha[*,†]

†*Theoretical and Computational Biophysical Chemistry Group, Department of Chemistry, Indian Institute of Technology Ropar, Rupnagar, 140001, Punjab , India*

‡*Department of Chemistry, GITAM School of Science, GITAM (Deemed to be University), Bengaluru 562163, India*

E-mail: sudipta@iitrpr.ac.in

Phone: +91-01881-232066

Introduction

The aggregation of the amyloid beta protein, a well-known neurodegenerative disease, causes Alzheimer's. Its pathology involves the formation of soluble oligomers and insoluble fibrils formation. The current understanding of AD research implies that the treatment of Alzheimer's patients should be focused on developing strategies to inhibit the growth of soluble oligomers/fibrils and disintegrate the already formed oligomers/fibrils simultaneously. Thus, a more realistic therapeutic approach should be to develop methods to ensure that Aβ peptide will exist in its non-toxic monomeric form, disintegrating the oligomers/fibrils. Lipopeptide-based nanomaterials derived from naturally occurring biological building blocks have received significant attention in AD research owing to their safety, biodegradability, and

biocompatibility.[S1,S2] For instance, Bera et al.[S3] in their recent spectroscopic and microscopic investigation illustrated that myristoyl-KPGPK lipopeptide-based nanovesicle dramatically hinders the random coil to β-sheet transformation of transmembrane GxxxGxxxGxxxG motif of Aβ-protein and human myelin protein zero, a prerequisite for the oligomerization of the peptide. Förster resonance energy transfer (FRET) assay performed with synthesized Cy-3 (FRET donor) and Cy-5 (FRET acceptor)-conjugated peptide further confirms that the nanovesicle strongly inhibits the fibril formation of the peptide.

Furthermore, this study highlighted that a suitable balance between the hydrophilic and hydrophobic nature of the nanovesicle is necessary for the inhibition. While this could serve as an essential insight for clinically viable drug design, the study should have addressed some critical questions necessary for further testing the clinical efficiency of this nanovesicle. For example, they experimented with the monomeric form peptide to test the nanovesicle's inhibition effect. While this confirms the inhibition of oligomerization event starting from the monomer, it cannot guarantee whether this nanovesicle can disintegrate the already formed oligomer, which is an important criterion to be a clinically viable AD drug. Therefore, it is worthwhile to probe (i) whether such a nanovesicle can disintegrate an already-formed oligomer and (ii) the molecular origin behind the inhibition by the nanovesicle.

Theoretical Background

Mean Field Model:

Our model system is composed of n spins, denoted by $S_1, S_2 ... S_n$ and their states are defined by two numbers, +1 and -1, for free and aggregate conditions. The following Ising model gives the energy function for these interacting spins

$$H = -\sum_{i} \epsilon_i S_i + \sum_{ij;\ i \neq j} J_{ij} S_i S_j = -\sum S_i E_i \tag{1}$$

where the term ϵ_i is the energy of the i_{th} unit, J_{ij} is the cooperative strength between two nearest spins, and $E_i = \epsilon_i + \sum J_{j\neq j} S_j$. These spins are harmonically coupled with a heat bath that allows the monomers orient and then form desired hydrogen bonds with their neighbours to form an aggregate. The evolution of the spins for this system can be written by a master equation as

$$\begin{aligned}\frac{d}{dt}P(S_1, S_2...S_n, t) = &- \sum W(S_i \to -S_i)P(S_1, S_2...S_i..S_n, t) \\ &+ \sum W(-S_i \to S_i)P(S_1, S_2... - S_i..S_n, t)\end{aligned} \tag{2}$$

where P is the joint probability and W is the transition matrix elements. Since we are interested in the equation of motion for the average value ($< S_i >= \sum_{S_i} S_i P(S_1, S_2...S_n, t)$) of the i_{th} spin or order parameter, we multiply the S_i on both of the sides of the 2 and then sum over all configurations reduces to the following equation of motion (EOM)

$$\frac{d}{dt} < S_i >= -2 < W(S_i \to -S_i)S_i > \tag{3}$$

If we assume the given process is a Markov process, then the transition matrix elements (TME) are given by the Golden rule.

$$W(S_i \to -S_i) = \frac{2\pi}{\hbar} \sum_{\alpha,\beta}^{\alpha\neq\beta} |F_{\alpha\beta}|^2 \rho_\beta \delta(-2E_i S_i + E_{\beta\alpha})$$

$$W(-S_i \to S_i) = \frac{2\pi}{\hbar} \sum_{\alpha,\beta}^{\alpha\neq\beta} |F_{\alpha\beta}|^2 \rho_\beta \delta(2E_i S_i + E_{\beta\alpha})$$

where the $\hbar$ is the Planck's constant by 2π, α, β are the bath states, F is the force acting on the system by the bath, ρ_β is the equilibrium probability for the bath. The Dirac δ function is introduced to describe the Markov process, $2E_i$ is the change in energy due to the flipping of spins and $E_{\beta\alpha} = E_\beta - E_\alpha$ is the energy gap between two bath states. Upon substitution

of these TMEs into the EOM, we obtain

$$\tau_i \frac{d}{dt} < S_i >= - < S_i > + \tanh(\frac{< E_i >}{k_B T}) \tag{4}$$

where the symbol $\tau_i^{-1} = \sum_{\alpha,\beta}^{\alpha \neq \beta} |F_{\alpha\beta}|^2 \rho_\beta [\delta(-2 < E_i > + E_{\beta\alpha}) + \delta(2 < E_i > + E_{\beta\alpha})] = \tau_{if}^{-1} + \tau_{ib}^{-1}$. Since we assume the heat bath is a collection of classical oscillators that couple with the spins to change its state from +1 to -1. Use of the integral form of the Dirac δ function, the transition matrix under the classical limit is

$$W(S_i \rightarrow -S_i) = \frac{|F|^2}{\hbar} \frac{\sqrt{\pi}}{\sqrt{\lambda k_B T}} e^{-\frac{(-2 < E_i > + \lambda)^2}{4 \lambda k_B T}}$$
$$W(-S_i \rightarrow S_i) = \frac{|F|^2}{\hbar} \frac{\sqrt{\pi}}{\sqrt{\lambda k_B T}} e^{-\frac{(2 < E_i > + \lambda)^2}{4 \lambda k_B T}}$$

The above transition matrix elements are also known as Marcus's result, where the $\lambda =< E_{\beta\alpha} >$ is usually called the reorganization energy, which is the energy to be dissipated on the aggregates free energy surface if the $< S_j >$ changes its value from +1 to -1. It has a significance that connects with the change in the heat bath energy ongoing from +1 to -1 spin states. Since Aβ aggregates form due to forming a few lateral hydrogen bonds, we consider them as reorganization energy. The explicit form this energy is $\sum_j \frac{\gamma_j^2}{\omega_j^2} d_j^2$, where γ_j is the coupling constants, ω_j frequency of the bath oscillator, $d_j =< S_j >_{+1} - < S_j >_{-1}$ is the displacement of the oscillators. Expressing the $< S_i >$ in terms of the mole fractions of the aggregate $x_i = (1 - < S_i >)/2$, the EOM becomes

$$\tau_i \frac{dx_i}{dt} = -x_i + \frac{1}{2} - \frac{1}{2} \tanh [\ \frac{\epsilon + 2J(1 - 2x_i)}{k_B T}] \tag{5}$$

Immediately, the mole fractions of the aggregates at equilibrium is

$$x_i^{eq} = \frac{1}{2} - \frac{1}{2} \tanh [\ \frac{\epsilon + 2J(1 - 2x_i^{eq})}{k_B T}] \tag{6}$$

If we consider all the spins are equivalent and their interactions happen only by the nearest neighbour interactions, then we can write $< E_i >= \epsilon + 2J < S >$. The above equations have several advantages, as we can modify the $< E_i >$ by defining an arbitrary model. Munoz-Eaton (ME) model is one example that can be incorporated easily into the model. Further, the environment of the peptides modifies their interactions, which can be included through the modifications of the ϵ. For example, we assume the effect of temperature and the crowder through the following linear modifications of the ϵ as

$$\epsilon = \epsilon^0 + \Delta\epsilon_T(T - T_0) \qquad \text{(Temperature effect)}$$

$$\epsilon = \epsilon^0 + \Delta\epsilon_C C_c \qquad \text{(Crowder effect)}$$

where ϵ_0 is the unperturbed internal interactions; T and C_c are the temperature and the concentrations of the crowders; and $\Delta\epsilon$ is the gradient of energy. The above model provides a comprehensive view of the nucleation-growth aggregation kinetics and the critical size of a nucleate as a function of cooperative interaction J, T and the crowder's effect.

Simulation Details

The initial structure file of Aβ_{17-42} was obtained in pentameric form from the protein data bank by PDB entry 2BEG.[S4] The disordered region that corresponds with the missing residues from 1 to 16 of the peptide is ignored from our model system because they do not have any significant role in amyloid formation. Octamer was prepared from this pentameric form of Aβ_{17-42} by placing the required number of hairpins along the z-axis. Not only octamer, but we also prepared a series of monomeric systems containing eight Aβ_{17-42} monomers placed randomly in a box. 17th (Leu) and 42nd (Asp) residues were capped with the standard ammonium and carboxylate ions. We added water molecules to the system and removed a water shell of $2\mathring{A}$ from the protein surface. We add 8 Na^+ ions randomly to neutralize the solvated system.

We carried out all-atom explicit-water MD simulations for Aβ_{17-42} octamer and their monomers placed randomly in the simulation box. We use Gromacs package version 2020.3 with CHARMM36 all-atom force field[S5]and the SPC water model[S6] under the NPT ensemble to simulate our systems. The Berendsen thermostats[S7] and Parrinello-Rahman barostat[S8] were applied to describe the constant temperatures and pressure of 1 atm. To study the effect of local heating, we set up five different simulations by increasing the kinetic energies of all the atoms of β-sheet fragment (25-37) of the $A\beta_{17-42}$ peptide. We change the kinetic energies of all those atoms by choosing the velocities of those atoms at 200K, 300K, 400K, 500K, and 600K. For that purpose, we use two Berendsen thermostats that maintain the specified temperature of the β sheet fragment and 300 K for the rest of the system, including water and ions.[S7] To explore the effect of SDS surfactants on amyloid aggregation, we prepared five more systems by adding 50, 100, 200, 300, and 400 SDS molecules. We add 5333, 4670, 3418, 2268, and 1315 water molecules to those systems. We calculate the Vander Waals(vdW) interactions by taking a cut-off of 1.0 nm and electrostatic interactions using the particle-mesh Ewald(PME) method with a grid spacing of 0.10 nm.[S9] We use the LINCS algorithm to constrain all bonds involving the hydrogen atoms[S10] and the Periodic Boundary Conditions (PBC) to remove the surface effects. We use the leapfrog algorithm and a timestep of 2 fs for solving the equation of motion.[S11] We performed MD simulations for 750 ns for each of the systems, with an equilibration period of 100 ns. The last 500 ns trajectories were used to obtain the average properties of the system.

Metadynamics

We performed a Well-Tempered metadynamics (WTMetaD) simulation using the GROMACS package patched with PLUMED.[S12] WTMetaD is an enhanced sampling technique used to build a free energy landscape for the structural changes of the Aβ_{17-42} octamer. WTMetaD has advantages over metadynamics simulation since the former converges to an exact value but fluctuates around the correct result as similar-sized Gaussians are deposited

along the CV. In this simulation, the sampling is enhanced by adding history-dependent bias potential.[S13] This bias potential is constructed in the free energy surface as a function of some order parameter called Collective variables (CVs). We choose the, C_α contact number (N_{C_α}) and radius of gyration (R_g) CVs for our simulation. We choose them because our primary aim is to obtain free energy cost for disrupting the amyloid aggregates.[S14] A biased potential is added in the form of Gaussian potential, V_b , for a WTMetaD simulation in the following way

$$V_b(s,t) = \sum_{t'=\tau_G,2\tau_G,..t'<t} w(t') e^{(\frac{-|s-s(t')|^2}{2\sigma^2}) - V_b(s(t),t')/k_B\Delta T} \tag{7}$$

where w and σ are height and width parameters defining the Gaussian potentials added at a time interval of τ. The factor, $e^{-V_b(s(t),t')/k_B\Delta T}$ scaled down the values of w, where the bias potential has been evaluated at the same point where the Gaussian is centered and ΔT is an input parameter related by $\gamma T - T$ and it is measured in temperature units. The free energy is obtained in the following way

$$F(s) = -(1 - \frac{1}{\gamma})V_b(s, t \to \infty) + C \tag{8}$$

where C is an arbitrary constant and $(1 - \frac{1}{\gamma})$ is the bias factor. All of these four parameters are sensitive to the free energy landscape. We optimized them and chose the Gaussians of height 2 kJ/mol, widths 3 and 0.1 nm for N_{C_α} and R_g CVs, and the values of γ is chosen as 15 respectively in our simulation. We deposit the V_b at every τ_G=50 ps and perform the simulation for about 1750 ns. The V_b perturbs the system away from any local minima and allows it to explore in complete phase space. As the simulation progresses, the bias potential converges to this negative free energy in equation 8 for a long time. Therefore, a long simulation allows us to explore any relevant energy basins. We choose the value of T=300 K for the entire WTMetaD simulation.

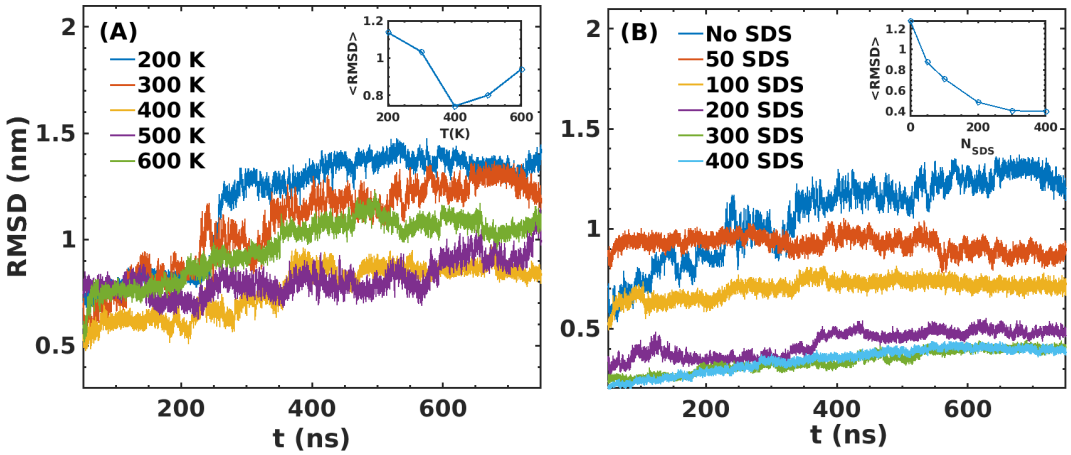

Figure S1: RMSD of the Aβ octamer as simulation progress. A) RMSD of Aβ octamer obtained from local heating of peptide. Inset figure shows $< RMSD >$ as a function of T. B) RMSD of Aβ octamer obtained from the simulation of Aβ octamer at various SDS molecules. Inset figure shows $< RMSD >$ as a function of N_{SDS}.

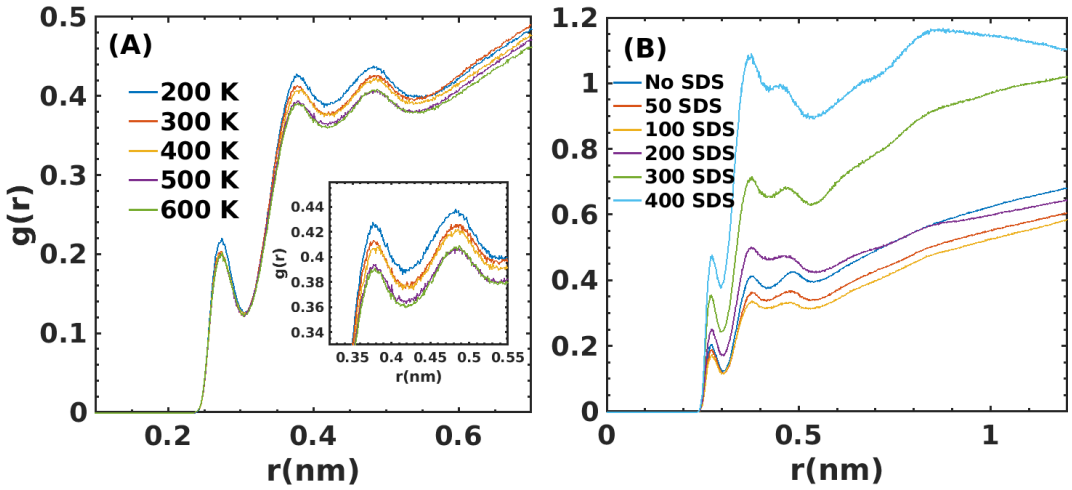

Figure S2: Radial distribution function (RDF)of water molecules around the Aβ octamer. A) RDF of Aβ octamer upon local heating of peptide. The inset figure shows RDF in the hydration shell at 0.37 nm and 0.49 nm. B)RDF of Aβ octamer in the presence of a number of SDS molecules.

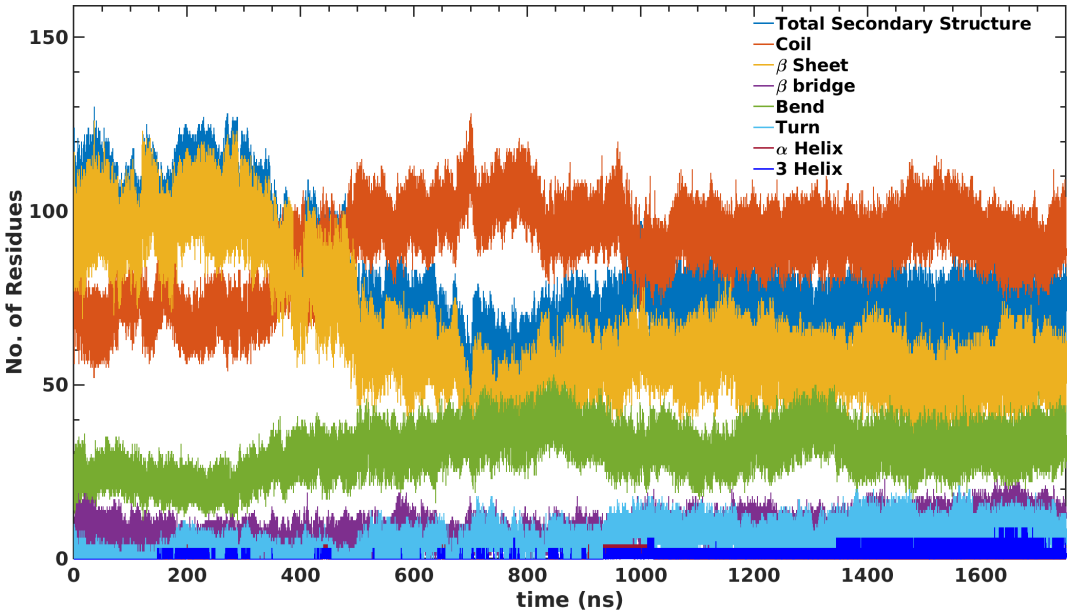

Figure S3: The secondary structures content of Aβ octamer during the metadynamics simulation of Aβ using two collective variables, namely R_g and N_{C_α}.

Parameters extracted from second barrier:

We extract the parameters from the second barrier of the minimum free energy landscape from the states C, E, and F, as shown in panel B of Figure 5 of the main text. The estimated barrier heights $\Delta G^{\dagger}$ for the forward and backward transitions are 27.28 kJ/mol and 31.27 kJ/mol. The free energy difference between the two states is ΔG_0 =-3.79 kJ/mol. According to our model, the $\Delta G_0 = 2\epsilon$ estimates the average interaction energy, ϵ =-1.895 kJ/mol. The obtained λ values for the forward and backward directions are 0.1224 kJ/mol and 0.1084 kJ/mol, respectively. The time for the forward and backward reactions are $\tau_f^{-1} = 5.4979 \times 10^{-2}$ s^{-1}, and $\tau_b^{-1} = 5.1648 \times 10^{-2}$ s^{-1} respectively. The calculated τ value for the second transition is 8.58 s.

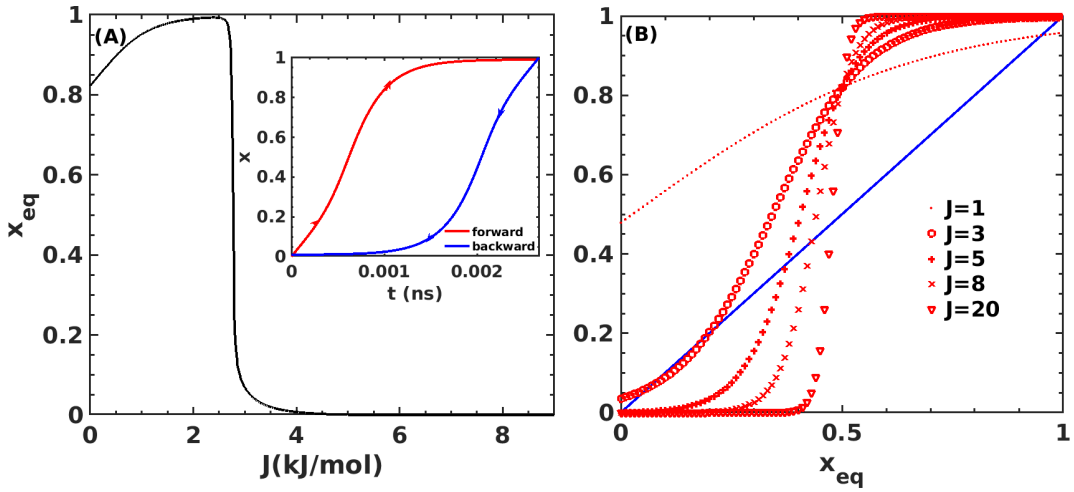

Figure S4: A) Variation of x_{eq} with coupling parameter, J. Inset figure represents the formation of hysteresis loop during the forward process, i.e., aggregate to the free state, and backward process, i.e., free state to aggregated state. B) Graphical solution of equation(6) for second barrier where $f_1(x_{eq}) = \frac{1}{2} - \frac{1}{2}\tanh\left[\frac{\epsilon+2J(1-2x_{eq})}{k_BT}\right]$ and $f_2(x_{eq}) = x_{eq}$.

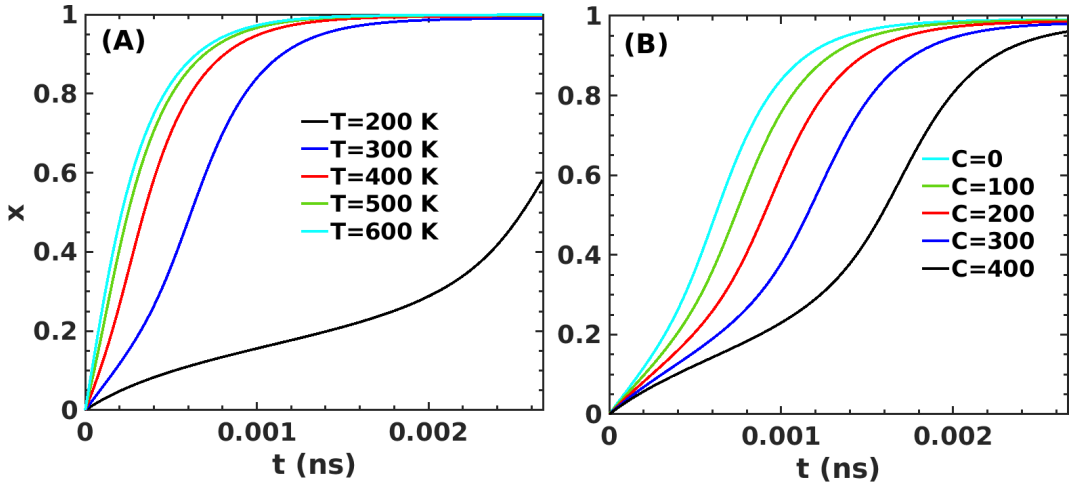

Figure S5: The Variation of x for the second barrier, i.e., from state C to G in figure 5B of main text as a function of time for J=3 kJ/mol with having $\epsilon_0 = -1.9$ kJ/mol A) at several temperatures B) at several concentrations of crowder.

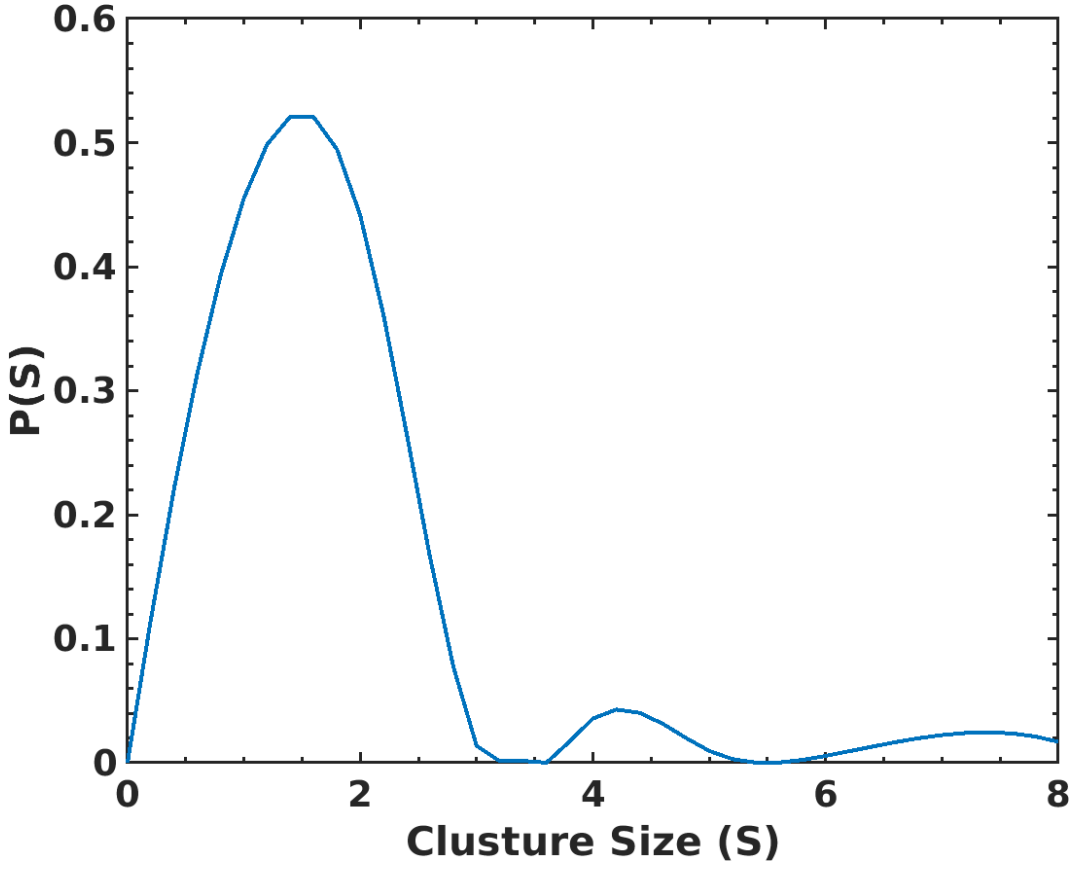

Figure S6: The probability distribution,P(S), of cluster size of Aβ oligomers obtained from the metadynamics simulation of Aβ using two collective variables, namely R_g and N_{C_α}.

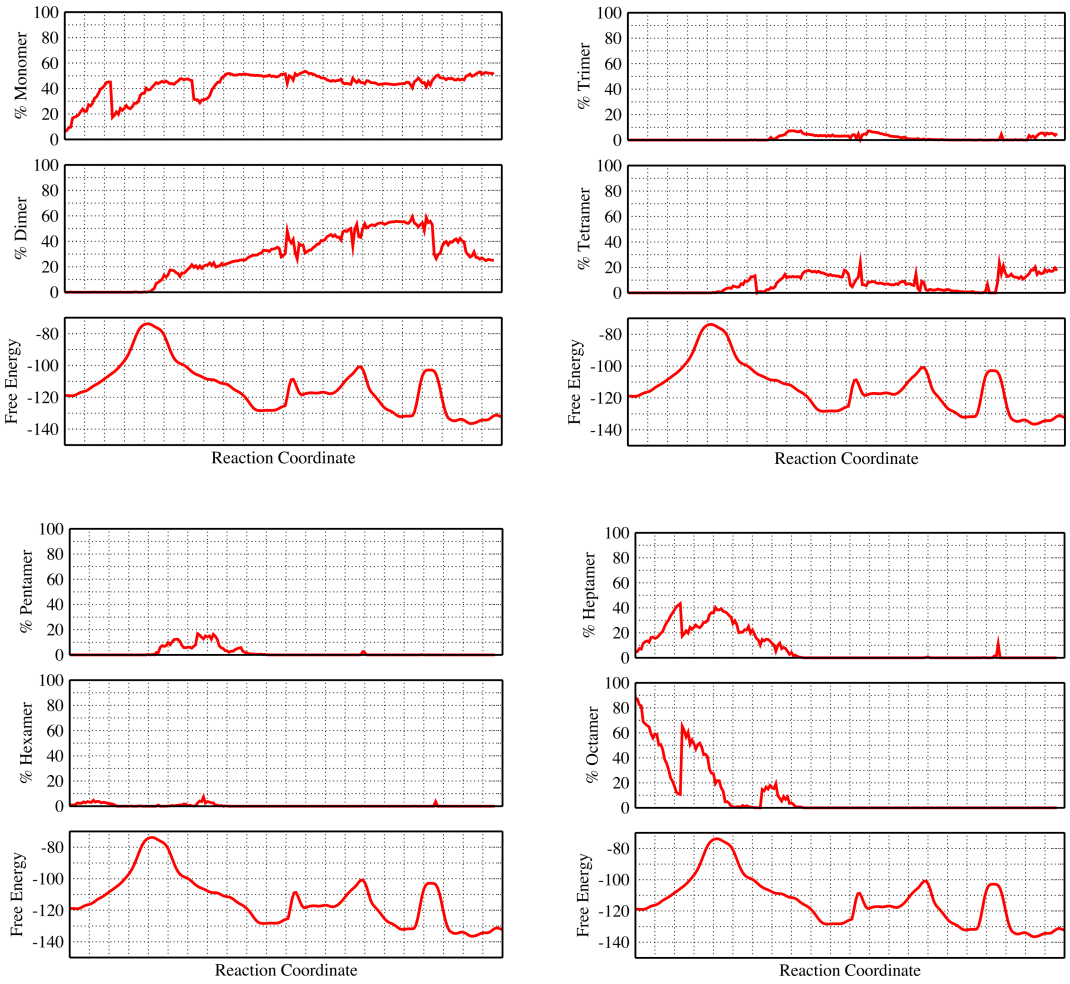

Figure S7: Free energy and the % of monomer, dimer, tetramer, pentamer, hexamer, heptamer, and octamer are shown as a function of order parameters. We use metadynamics trajectory for this analysis.

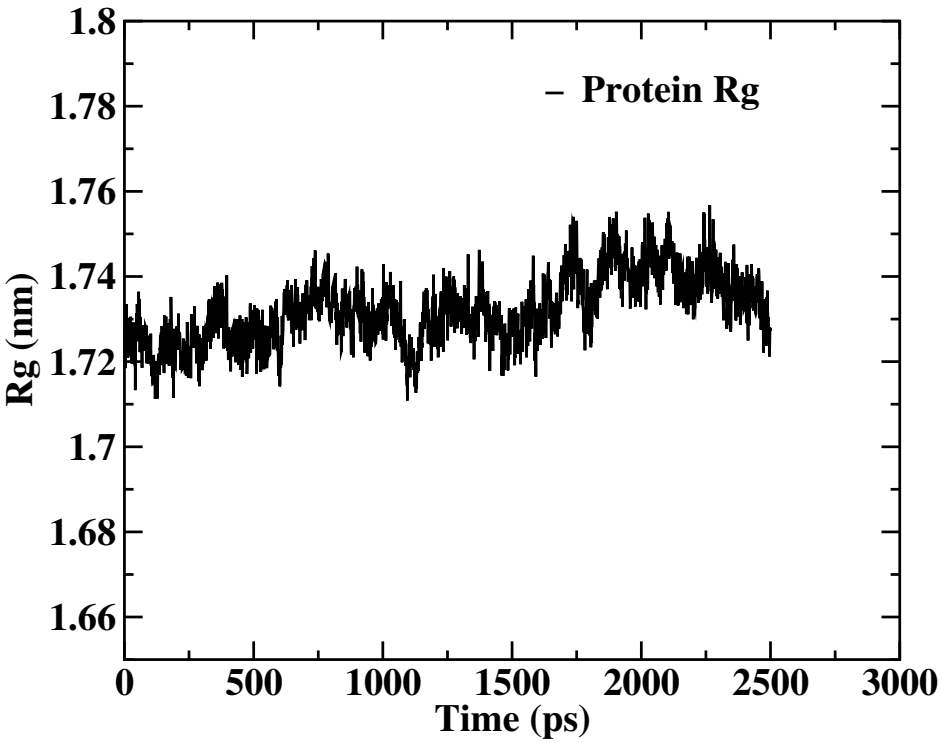

Figure S8: Radius of gyration for stable amyloid octamer

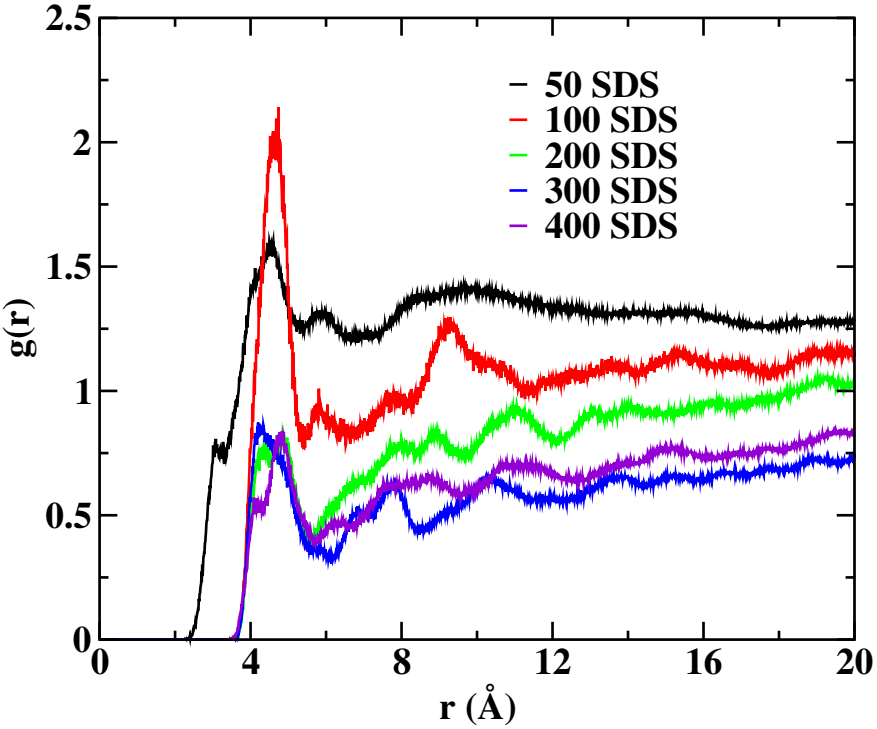

Figure S9: Radial distribution function for SDS around the amyloid octamer

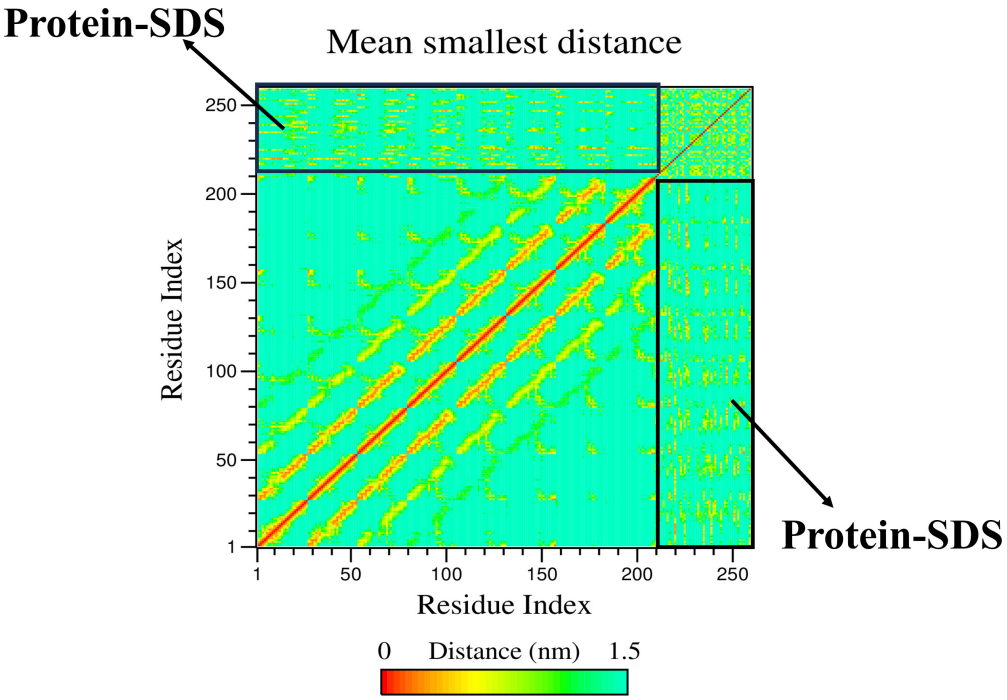

Figure S10: Contact map between Protein-SDS in the case of amyloid octamer with 50 SDS. Regions highlighted within the rectangular box represent the Protein-SDS contact.

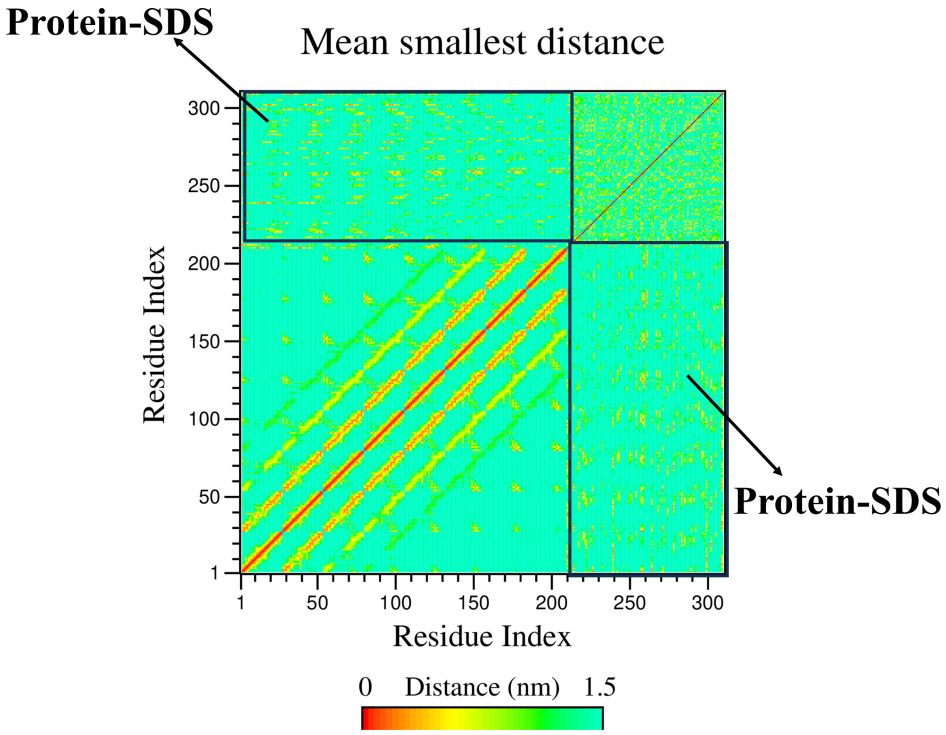

Figure S11: Contact map between Protein-SDS in the case of amyloid octamer with 100 SDS. Regions highlighted within the rectangular box represent the Protein-SDS contact.

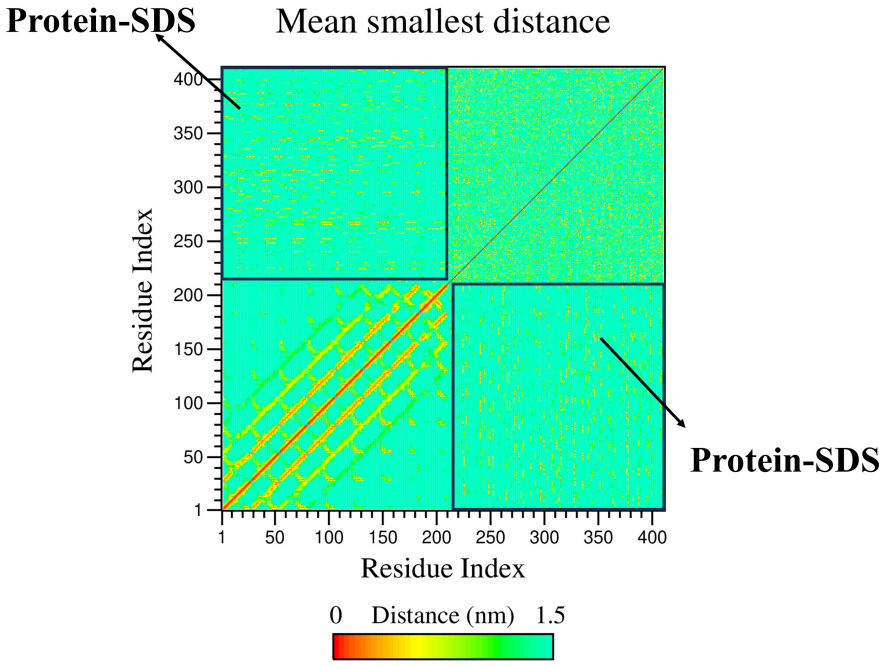

Figure S12: Contact map between Protein-SDS in the case of amyloid octamer with 200 SDS. Regions highlighted within the rectangular box represent the Protein-SDS contact.

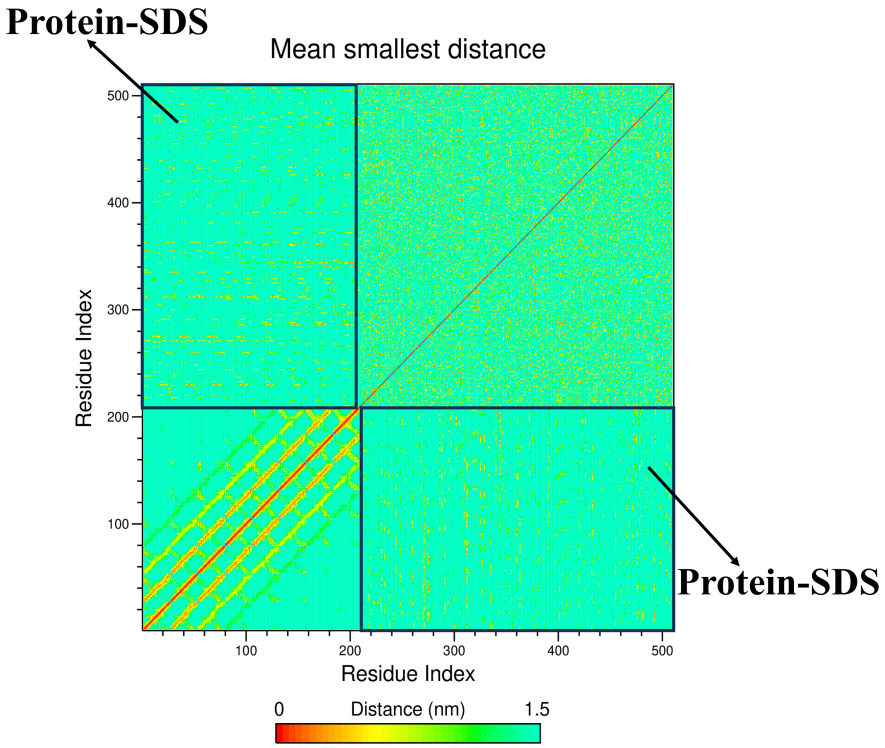

Figure S13: Contact map between Protein-SDS in the case of amyloid octamer with 300 SDS. Regions highlighted within the rectangular box represent the Protein-SDS contact.

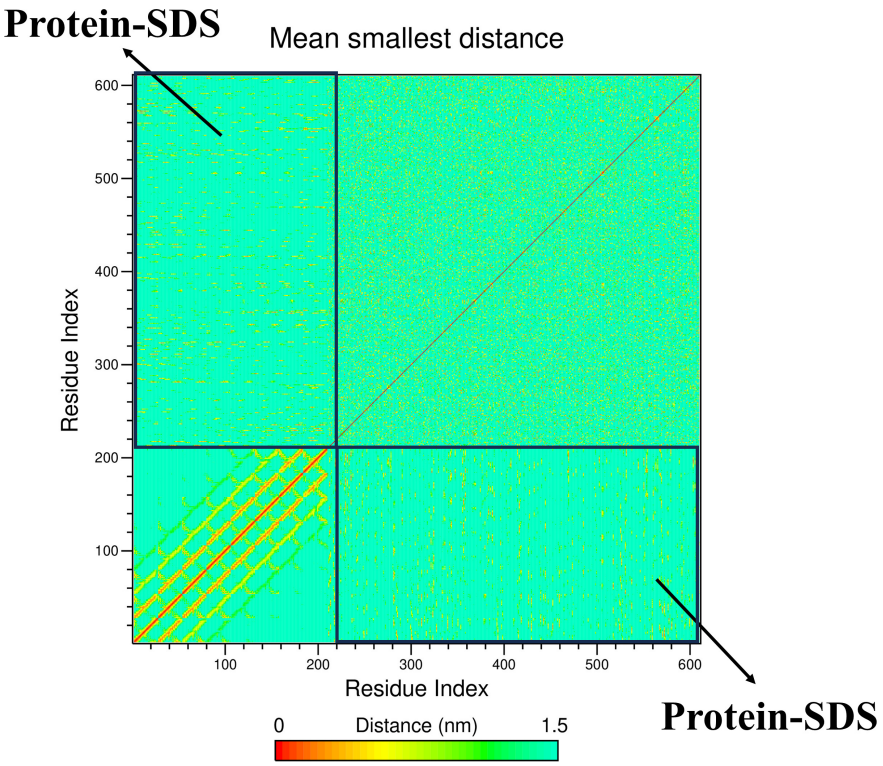

Figure S14: Contact map between Protein-SDS in the case of amyloid octamer with 400 SDS. Regions highlighted within the rectangular box represent the Protein-SDS contact.

References

(S1) Levin, A.; Hakala, T. A.; Schnaider, L.; Bernardes, G. J.; Gazit, E.; Knowles, T. P. Biomimetic peptide self-assembly for functional materials. *Nature Reviews Chemistry* **2020**, *4*, 615–634.

(S2) Wei, G.; Su, Z.; Reynolds, N. P.; Arosio, P.; Hamley, I. W.; Gazit, E.; Mezzenga, R. Self-assembling peptide and protein amyloids: from structure to tailored function in nanotechnology. *Chemical Society Reviews* **2017**, *46*, 4661–4708.

(S3) Bera, T.; Saha, P. C.; Chatterjee, T.; Kar, S.; Guha, S. Construction of Self-Assembling Lipopeptide-Based Benign Nanovesicles to Prevent Amyloid Fibril Formation and Reduce Cytotoxicity of GxxxGxxxGxxxG Motif. *Bioconjugate Chemistry* **2022**,

(S4) Luhrs, T.; Ritter, C.; Adrian, M.; Riek-Loher, D.; Bohrmann, B.; Dobeli, H.; Schubert, D.; Riek, R. 3D structure of Alzheimer's amyloid-β(1-42) fibrils. *Proc. Natl. Acad. Sci. U.S.A.* **2005**, *102*, 17342–17347.

(S5) Huang, J.; Jr, A. D. M. CHARMM36 All-Atom Additive Protein Force Field: Validation Based on Comparison to NMR Data. *J. Comput. Chem* **2013**, *34*, 2135–3145.

(S6) .Berendsen, H. J. C.; J.P.M.Postma; Gunsteren, W.; .Hermans, J. Interaction models for water in realtion to protein hydration. *Intermolecular Forces* **1981**, 331–342.

(S7) Berendsen, H. J. C.; Postma, J. P. M.; van Gunsteren, W. F.; DiNola, A.; Haak, J. R. Molecular dynamics with coupling to an external bath. *J. Chem. Phys.* **1984**, *81*, 3684–3690.

(S8) M.Parrinello; A.Rahman Polymorphic transitions in single crystals: A new molecular dynamics method. *J. Appl. Phys.* **1981**, *52*, 7182–7190.

(S9) Darden, T.; York, D.; Pedersen, L. Particle mesh Ewald: An N.log(N) method for Ewald sums in large systems. *J. Chem. Phys.* **1993**, *98*, 10089–10092.

(S10) Hess, B.; bekker, H.; Berndsen, H. J. C.; Fraaije, J. G. E. M. LINCS: A Linear Constraint Solver for Molecular Simulations. *J. Comput. Chem.* **1997**, *18*, 1463–1472.

(S11) Hockney, R.; S.P.Goel; Easwald, J. Quiet High-Resolution Computer Models of a Plasma. *J. Comput. Phys.* **1974**, *14*, 148–158.

(S12) Bonomi, M.; Branduardi, D.; Bussi, G.; Camilloni, C.; Provasi, D.; Raiteri, P.; Donadio, D.; Marinelli, F.; Pietrucci, F.; Broglia, R. A.; Parrinello, M. PLUMED: A portable plugin for free-energy calculations with molecular dynamics. *Comput. Phys. Commun* **2009**, *180*.

(S13) Barducci, A.; Bonomi, M.; Parrinello, M. Metadynamics. *Wiley Interdiscip. Rev. Computat. Mol. Sci.* **2011**, *1*, 826–843.

(S14) Baftizadeh, F.; Biarnes, X.; Pietrucci, F.; Affinito, F.; Laio, A. Multidimensional view of amyloid fibril nucleation in atomistic detail. *Journal of the American Chemical Society* **2012**, *134*, 3886–3894.